Polarization change in ferroelectric thin film capacitors under external stress

H. Zhu,[1] D. P. Chu,[1,a)] N. A. Fleck,[2] S. E. Rowley,[3] and S. S. Saxena[3]
[1]*Electric Engineering Division, University of Cambridge, 9 JJ Thomson Avenue, Cambridge CB3 0FA, United Kingdom*
[2]*Department of Engineering, University of Cambridge, Cambridge CB2 1PZ, United Kingdom*
[3]*Cavendish Laboratory, University of Cambridge, Cambridge CB3 0HE, United Kingdom*

(Received 30 June 2008; accepted 2 February 2009; published online 16 March 2009)

The changes in polarization and coercive voltage of lead zirconate titanate (PZT) thin film of 130 nm in thickness were measured under hydrostatic pressure up to 1.5 GPa. By converting the isotropic loading to an equivalent out-of-plane uniaxial compressive loading, it was found that these results were consistent with our previous results of uniform in-plane tensile stress, showing that the polarization changes under these two different loading conditions are of the same nature. The combined results demonstrate that the intrinsic polarization decreased linearly with the level of stress at a rate of -0.013 $\mu C\ cm^{-2}\ MPa^{-1}$ with a critical stress of 1.6 GPa to paraelectric phase. Further comparison of our result with that of a thick PZT film and bulk PZT materials suggests that ferroelastic switching (90° switching) is dominant in the bulk material, and the polarization reduction in our thin film is due to material intrinsic lattice distortion under pressure, while the thick film response is intermediate. The effect of substrate clamping on ferroelastic domains is also shown. © *2009 American Institute of Physics*. [DOI: 10.1063/1.3089303]

I. INTRODUCTION

Ferroelectric thin films have a wide range of applications because of the strong couplings between their electrical, mechanical, and thermal properties. The electrical property of polarization has been investigated intensively for the application of nonvolatile memory devices.[1,2] Other properties, such as piezoelectric and pyroelectric characteristics, have also been studied for sensors, actuators, and infrared detectors.[3,4]

Ferroelectric thin films deposited on stiff substrate are usually subjected to in-plane residual stress due to the difference between the thermal expansion coefficients of ferroelectrics and substrate material. Such an in-plane residual stress is usually on the order of a few hundreds of megapascals.[5,6] Ferroelectric thin film capacitor stacks are also often subject to out-of-plane stress, as a result of deposition of passivation layer, and the level of induced out-of-plane stress can be up to gigapascal order.[7] Furthermore, in the integration of ferroelectric random access memory (FRAM), the stress that occurred during depositing the interlayer dielectrics (ILD) and interconnect metal layer is considered as one of the vital factors in degrading the ferroelectric property. It was observed that the ILD generates a compressive stress[8] and the interconnect metal layer generates a tensile stress on ferroelectric capacitors.[9] In particular, out-of-plane stress component (σ_{zz}) when a passivation layer was deposited was stated in the case of a single planar Pt electrode.[8] The ferroelectric capacitor stack can be considered as being under a hydrostatic stress condition.[8,10] The level of their stresses can be more pronounced for the ferroelectric thin film capacitor with the aspect ratio (width/height ~1) for modern FRAM than that of large size planar case, and the properties of ferroelectric thin film capacitors will be affected accordingly.

There have been detailed studies of the polarization changes of bulk lead zirconate titanate (PZT) materials under stress, which show that both saturation polarization (P_s) and remnant polarization (P_r) decrease rapidly if there is a compressive stress along the polarization direction.[11–14] Illustration of the effect of applied stress on the domain wall movement and change of polarization direction in different sample configurations can be found in Refs. 12–14. However, it is difficult to apply truly uniaxial stress to a thin film.[15] In 1965, Samara[16] used a hydrostatic-pressure apparatus and studied the polarization change of Rochelle salt and later the dielectric properties and phase transitions of ferroelectric perovskites.[17] Grishin *et al.*[18] applied hydrostatic pressure on a PZT film of 600 nm in thickness and found that the remnant polarization decreases monotonously with pressure up to 1 GPa. There were also investigations of the in-plane tensile stress effect on the polarization of PZT thin films.[19,20] However, their approaches could not ensure that the stress applied across the sample was uniform. Recently, we applied a uniform in-plane tensile stress up to 150 MPa to PZT thin film samples and found that the out-of-plane polarization decreases linearly with the level of applied stress,[21] similar to what was reported previously.[22] Nevertheless, there is no detailed study of the effect of significant mechanical loading on ferroelectric thin films of around 100 nm in thickness, which are of particular application interest for FRAMs. In addition, the investigations carried out so far only managed to show the effect of mechanical loading applied in a particular manner, either in plane or out of plane. A systematic study is lacking from the literature.

In this work, we will present our results on the changes

a)Author to whom correspondence should be addressed. Electronic mail: dpc31@cam.ac.uk.

of polarization and coercive voltage in a PZT thin film of 130 nm in thickness under hydrostatic pressure up to 1.5 GPa and compare them with our previous results of in-plane tensile stress. Taken together, the results for these two stress states provide us with a unified picture of polarization change under extrinsic stresses. Finally we will compare our results with that of a PZT film of 600 nm in thickness and that of bulk PZT material and discuss the link between the behaviors of polarization under pressure and the intrinsic polarization states of the samples, as well as the effect of substrate clamping.

II. EXPERIMENTAL APPROACH

A ferroelectric PZT thin film was deposited on a platinized Si substrate by the sol-gel method using a composition of $Pb(Zr_{0.45}Ti_{0.55})O_3$. The annealed film, with thickness of 130 nm, was in the polycrystalline tetragonal state with a dominant orientation of (111). The top Pt electrodes were square in plan view, with a side width of 46 μm, as described in our previous work.[21]

The hydrostatic pressure was supplied by a high-pressure cell. A sketch of the pressure cell is shown in Fig. 1(a). When the piston of the pressure cell is pushed down, the poly(tetrafluoroethylene) (PTFE) tube is compressed inside the pressure cylinder and a hydrostatic pressure is applied on the sample isotropically via the pressure transmitting fluid inside the tube. Figure 1(b) shows the hydrostatic pressure σ_{hy} applied on our PZT thin film sample; each layer is considered to be isotropic with the same value for the in-plane ($E_{\parallel}$) and out-of-plane ($E_{\perp}$) Young's moduli. The pressure is measured by a calibrated manganin resistance gauge with an accuracy of ± 0.05 GPa. Two insulated wires are connected to the top and bottom electrodes of the ferroelectric thin film capacitor, respectively, and led out of the pressure cell through a sealed feed to a Radiant Technology Precision Premiere Ferroelectrics tester for electrical measurements.

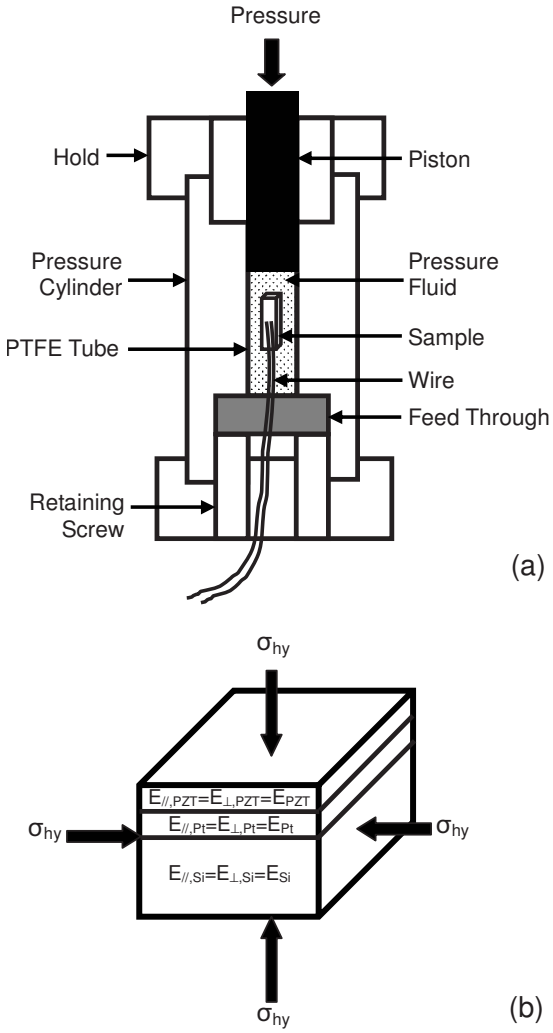

FIG. 1. Schematic diagram of (a) high-pressure cell and (b) hydrostatic pressure σ_{hy} on a PZT thin film sample with isotropic Young's modulus, i.e., $E_{\parallel}=E_{\perp}$ for all the materials.

III. RESULTS AND DISCUSSIONS

The hysteresis curves of our ferroelectric capacitor are shown in Fig. 2(a) for selected values of hydrostatic pressure. It is clear that the magnitude of charge density, D, decreases when the applied stress σ increases. Because the measured charge density, $D=\varepsilon_0\varepsilon_r E+P$, includes the contributions from both dielectric response and ferroelectric polarization switching, it is necessary to subtract the dielectric part from the overall charge density for polarization. This is not the usual procedure, as in normal measurement conditions the dielectric part does not change noticeably. Polarizations shown in Fig. 2(b) are calculated from $P=D-CV/A$, where C is the dielectric capacitance from the linear part of hysteresis curve near the maximum applied voltages and A is the area of capacitor. The maximum polarizations, $P_{\pm,\max}$, are defined as the constant values at the maximum applied voltages, $\pm V_{\max}$. Similar as in our previous work,[21] we define the difference between the polarization under mechanical loading, $P(V,\sigma_{hy})$, and free state, $P(V,0)$, at different applied voltages, $\Delta P(V,\sigma_{hy})=P(V,\sigma_{hy})-P(V,0)$, and plot it in Fig. 3(a) for typical pressure levels. At any given σ_{hy}, $\Delta P(V,\sigma_{hy})$ approaches a constant value when the magnitude of applied voltage is large, namely, $\Delta P_+(\sigma_{hy})$ and $\Delta P_-(\sigma_{hy})$ in the positive and negative voltage regions, respectively. We believe that the polarization changes [$\Delta P_+(\sigma_{hy})$ and $\Delta P_-(\sigma_{hy})$] are a better and more reliable representation of the polarization state than that of the conventionally used remnant polarization change from a single voltage point.[12,19,21] To minimize the asymmetry between top and bottom electrodes due to the process difference, we use the average value, $\Delta P(\sigma_{hy})=[\Delta P_+(\sigma_{hy})-\Delta P_-(\sigma_{hy})]/2=k_{hy}(\sigma_{hy})$, as the overall change of polarization. Figure 3(b) shows that $\Delta P(\sigma_{hy})$ is independent of the maximum applied voltage; it decreases linearly with increasing hydrostatic pressure, with a zero intercept and $k_{hy}=-0.003$ μC cm^{-2} MPa^{-1}. Therefore, we can express the maximum polarization under pressure as $P_{\max}(\sigma_{hy})=P_{\max}(0)+\Delta P(\sigma_{hy})=k_{hy}(\sigma_{hy}-\sigma_{c,hy})$, where $P_{\max}(0)$ is the maximum polarization in free state, k_{hy} is the rate of change, and $\sigma_{c,hy}$ is the critical hydrostatic pressure to paraelectric state. Note that although $\Delta P(\sigma_{hy})$ (and k_{hy}) is independent of $V_{\max}$, $P_{\max}(0)$ (hence $\sigma_{c,hy}$) is not. In Fig. 4(a), $P_{\max}(\sigma_{hy})$ for $V_{\max}=3$ V is plotted alongside the rem-

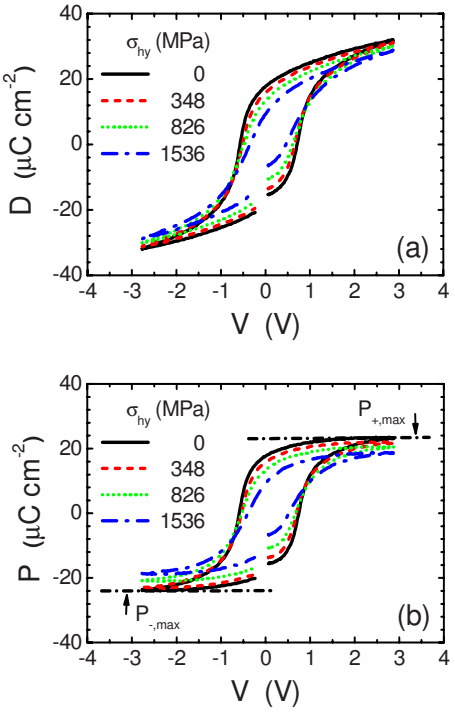

FIG. 2. (Color online) Hysteresis curves of (a) charge density and (b) polarization under typical hydrostatic pressures.

nant polarization under pressure, $P_r(\sigma_{\mathrm{hy}})$. If the same pressure dependence is used for both $P_{\max}(\sigma_{\mathrm{hy}})$ and $P_r(\sigma_{\mathrm{hy}})$, we can obtain $k_{\mathrm{hy}}=-0.003$ μC cm^{-2} MPa^{-1} and $\sigma_{c,\mathrm{hy}}=7.24$ GPa for $P_{\max}(\sigma_{\mathrm{hy}})$ and $k_{\mathrm{hy}}=-0.005$ μC cm^{-2} MPa^{-1} and $\sigma_{c,\mathrm{hy}}=3.37$ GPa for $P_r(\sigma_{\mathrm{hy}})$. The large critical stress for $P_{\max}$ is a function of the level of applied voltage, which will be discussed later.

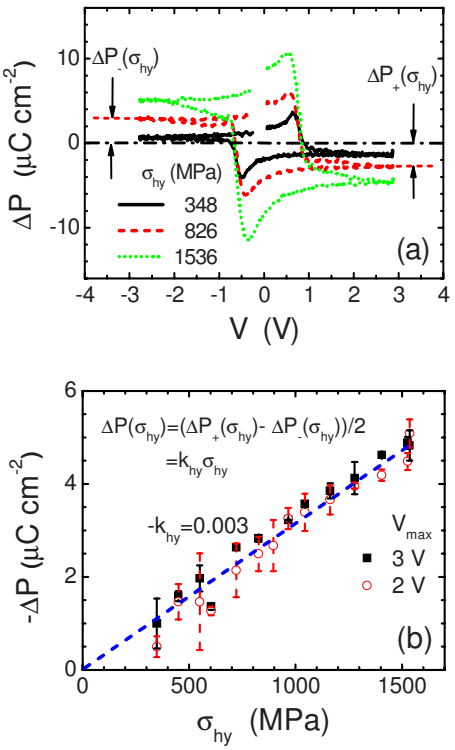

FIG. 3. (Color online) (a) Change of polarization $\Delta P(V,\sigma_{\mathrm{hy}})=P(V,\sigma_{\mathrm{hy}})-P(V,0)$ under typical hydrostatic pressures; (b) the overall polarization change $\Delta P(\sigma_{\mathrm{hy}})=[\Delta P_+(\sigma_{\mathrm{hy}})-\Delta P_-(\sigma_{\mathrm{hy}})]/2$ vs hydrostatic pressure σ_{hy}.

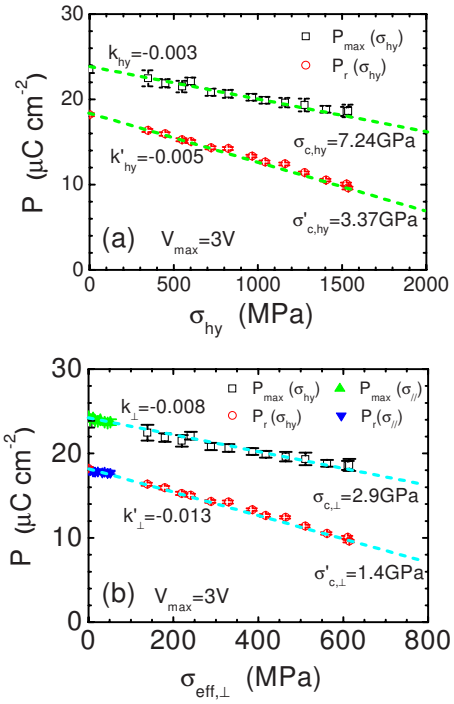

FIG. 4. (Color online) Maximum polarization $P_{\max}$ and remnant polarization P_r as a function of (a) hydrostatic pressure and (b) effective out-of-plane stress.

To be able to compare the results here to our previous results of in-plane stress, $\sigma_{\parallel}$, we would like to convert both $\sigma_{\parallel}$ and σ_{hy} to an effective out-of-plane stress, $\sigma_{\perp}$. From mechanics, we have $\sigma_{\perp}=\nu\sigma_{\parallel}$, where ν is the Poisson ratio of material. In the case of hydrostatic pressure, the bulk modulus K, which reflects the material resistance to change its volume under hydrostatic load, is defined as the ratio of hydrostatic pressure σ_{hy} to the relative volume change $\Delta V/V$ and can be related to the principle strains (ε_{xx}, ε_{yy}, and ε_{zz}),

$$K=\frac{\sigma_{\mathrm{hy}}}{\Delta V/V}=\frac{\sigma_{\mathrm{hy}}}{\varepsilon_{xx}+\varepsilon_{yy}+\varepsilon_{zz}}=\frac{E}{3(1-2\nu)}, \tag{1}$$

where E is Young's modulus of material. Since Young's moduli of PZT, Pt, and the Si substrate are approximately the same in value, $E_{\mathrm{PZT}}\sim 145-165$ GPa,[23] $E_{\mathrm{Pt}}\sim 170$ GPa, and $E_{\mathrm{Si}}\sim 130-170$ GPa,[24] respectively, we can treat our PZT thin film capacitor system simply as a mechanically isotropic system, which has the same principle strain under hydrostatic pressure as $\varepsilon_{xx}=\varepsilon_{yy}=\varepsilon_{zz}=\varepsilon=\sigma_{\perp}/E_{\mathrm{PZT}}$ and the equivalent out-of-plane stress as

$$\sigma_{\perp}=(1-2\nu)\sigma_{\mathrm{hy}}. \tag{2}$$

Using the above relationships between the in-plane tensile stress and hydrostatic pressure and the equivalent out-of-plane compressive stress, we can also express the critical stresses in these cases as $\sigma_{c,\perp}=\nu\sigma_{c,\parallel}=(1-2\nu)\sigma_{c,\mathrm{hy}}$. Giving the fact that the converted critical out-of-plane compressive stress should the same for both cases, we obtain the value of Poisson ratio $\nu=0.3$ for our PZT thin film sample. This value is consistent with that being used in literatures.[25,26]

The polarization changes in terms of the equivalent out-of-plane stress are shown in Fig. 4(b) for both hydrostatic

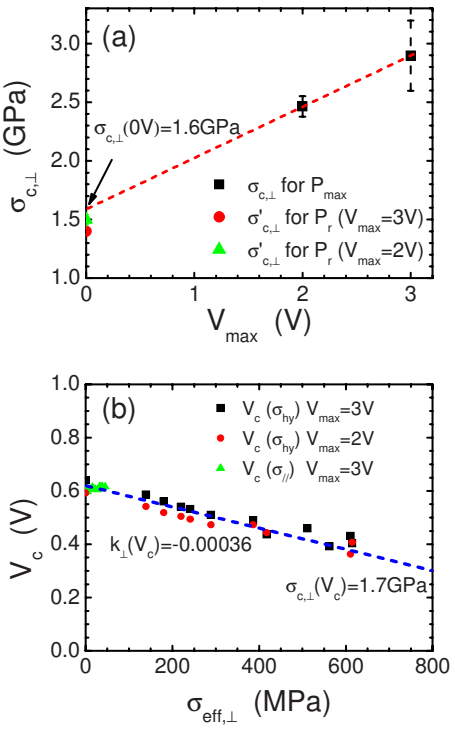

FIG. 5. (Color online) (a) Critical stress vs maximum applied switching voltage; (b) coercive voltage vs the effective out-of-plane stress with two different maximum applied switching voltages.

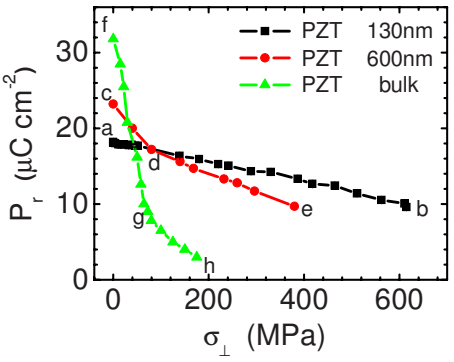

FIG. 6. (Color online) Remnant polarization vs out-of-plane compressive stress for bulk PZT (Ref. 9), thick (Ref. 10), and thin PZT film samples. The slopes of each linear section are $k_{ab}=-0.013$ μC cm^{-2} MPa^{-1}, $k_{cd}=-0.075$ μC cm^{-2} MPa^{-1}, $k_{de}=-0.025$ μC cm^{-2} MPa^{-1}, $k_{fg}=-0.320$ μC cm^{-2} MPa^{-1}, and $k_{gh}=-0.050$ μC cm^{-2} MPa^{-1}. The critical stresses derived from $P_r(\sigma_\perp)=k'_\perp(\sigma_\perp-\sigma'_{c,\perp})$ for each linear section are $\sigma_{ab}=1400$ MPa, $\sigma_{cd}=310$ MPa, $\sigma_{de}=772$ MPa, $\sigma_{fg}=100$ MPa, and $\sigma_{gh}=230$ MPa.

pressure and in-plane loading[21] cases. We can see that the two results agree very well with each other, which shows that the nature of the polarization change in these two different stress conditions is essentially the same. If using $P_{\max}(\sigma_\perp)=k_\perp(\sigma_\perp-\sigma_{c,\perp})$ and $P_r(\sigma_\perp)=k'_\perp(\sigma_\perp-\sigma'_{c,\perp})$ to describe the linear dependence on loading, we have $k'_\perp=-0.008$ μC cm^{-2} MPa^{-1} and $k'_\perp=-0.013$ μC cm^{-2} MPa^{-1} and critical stresses of $\sigma_{c,\perp}=2.9$ GPa and $\sigma'_{c,\perp}=1.4$ GPa, respectively.

Since the value of $P_{\max}$, hence $\sigma_{c,\perp}$, is dependent on the maximum applied voltage $V_{\max}$, we repeated the experiment with a different maximum applied voltage of 2 V. The critical stress $\sigma_{c,\perp}(2\ \mathrm{V})$ is 2.5 GPa for the maximum polarization, which is smaller than $\sigma_{c,\perp}(3\ \mathrm{V})=2.9$ GPa as shown in Fig. 4(b). This is probably a result due to the effects of stress and applied polarization voltage combined together. Although the polarization change ΔP depends only on the external stress, the actual polarization in stress condition is a competitive process between the electric energy and the elastic energy, which means that a large critical stress is required to overcome a large electric field to reach the paraelectric state. Figure 5(a) shows the converted critical out-of-plane compressive stresses at $V_{\max}=2$ and 3 V, together with that for remnant polarization. The extrapolation to $V_{\max}=0$ V gives a critical stress of $\sigma_{c,\perp}(0\ \mathrm{V})=1.6$ GPa, which is slightly higher than the critical stresses for remnant polarization P_r of $\sigma'_{c,\perp}(3\ \mathrm{V})=1.4$ GPa and $\sigma'_{c,\perp}(2\ \mathrm{V})=1.5$ GPa, respectively. It is reasonable to believe that $\sigma'_{c,\perp}$ will converge to $\sigma_{c,\perp}(0\ \mathrm{V})$ as the applied voltage is reduced to zero and, hence, the critical stress $\sigma_{c,\perp}(0\ \mathrm{V})$ is the intrinsic critical stress of material.

In addition to the change of polarization, we investigated the stress effect on the coercive voltage V_c for the ferroelectric thin film. We found that V_c also reduces linearly as the out-of-plane pressure increases, which can be expressed in the same way as $P_{\max}$ with an expression $V_c(\sigma_\perp)=k_\perp(V_c)\times[\sigma_\perp-\sigma_{c,\perp}(V_c)]$. The critical stress for V_c is deduced to be 1.7 GPa with a material intrinsic coercive voltage of 0.62V, as shown in Fig. 5(b). Our results show that the maximum applied voltage has little effect on the coercive field.

The microscopic origin of the decrease in polarization and coercive voltage under external stress can be easily understood in terms of the potential double well model for ferroelectrics. When a PZT material is subjected to external compressive stress, the equilibrium position of Ti/Zr ions moves toward the center of a unit cell, hence the reduction in polarization and potential barrier height (the microscopic coercive field) as demonstrated by first-principles calculations.[27] However, this model can only lead to a single dependence of polarization on external stress, which is not sufficient to explain the results of real situations.

In the macroscopic scale, the decrease in polarization in bulk PZT materials can be understood in terms of ferroelectric switching (180° switching) and ferroelastic switching (90° switching) under applied electrical and mechanical loadings.[12] To apply a uniaxial loading will cause ferroelastic switching of polarization to a direction away from the loading axis, hence the reduction in remnant polarization component in the loading direction. In Fig. 6, we plotted the out-of-plane remnant polarization as a function of effective out-of-plane compressive stress in three systems of different geometries: bulk ceramic PZT,[12] 600 nm thick PZT film,[13] and our 130 nm thick PZT film. They are a poled soft ferroelectric ceramics $Pb(Zr_{0.52}Ti_{0.48})O_3$ (PZT-5*H*), (001) oriented $Pb(Zr_{0.52}Ti_{0.48})O_3$ thick film on single crystal $LaAlO_3$ substrate and (111) oriented $Pb(Zr_{0.45}Ti_{0.55})O_3$ thin film on silicon wafer, respectively. Although they are of different compositions and crystalline orientations, it is clear that P_r in all cases have a linear dependence on $\sigma_\perp$ and can be represented by using an expression $P_r(\sigma_\perp)=k'_{c,\perp}(\sigma_\perp-\sigma'_{c,\perp})$. However, there are two linear sections in the case of bulk

PZT and 600 nm thick PZT films, with a fast decreasing section in the low pressure range, while there is only one slow decreasing section for the whole pressure range in the case of the 130 nm thick PZT film. $k'_{\perp}$ and $\sigma'_{c,\perp}$ of the two sections are -0.320 and -0.050 $\mu C\,cm^{-2}\,MPa^{-1}$ and 100 and 230 MPa for the bulk PZT film, and -0.075 and -0.025 $\mu C\,cm^{-2}\,MPa^{-1}$ and 310 and 772 MPa for the 600 nm thick PZT film, respectively. For the 130 nm thick film, $k'_{\perp}$ and $\sigma'_{c,\perp}$ are -0.013 $\mu C\,cm^{-2}\,MPa^{-1}$ and 1400 MPa, respectively. We suggest that the section with the larger slope is associated to the response of ferroelastic switching, while the one with the smaller slope is associated to the response of lattice distortion under loading. This agrees with the statements that the volume fraction of polarization along the poling direction is usually dominant in a poled bulk ferroelectric material and it reduces due to ferroelastic switching first before undergoing further reduction in polarization under pressure. The short section of larger slope in 600 nm thick film shows a reduced volume fraction of polarization along the poling direction as geometry changes from bulk to film. For the thin film of 130 nm in thickness, there is only a single section of polarization reduction with a constant small slope due to lattice distortion because of the high residual stress in the film and substrate clamping effect. This is consistent with the fact that the polarization change has the same dependence on pressure in both cases of in-plane stress in low pressure range and hydrostatic loading in high-pressure range, as shown in Fig. 4(b). The slope of our sample under in-plane tensile stress (-0.0023 $\mu C\,cm^{-2}\,MPa^{-1}$) (Ref. 21) also agrees with the previous modeling result (~ -0.0028 $\mu C\,cm^{-2}\,MPa^{-1}$),[22] supporting that of only lattice distortion without ferroelastic switching. The possibility of observing the material intrinsic property of lattice distortion under pressure is probably due to the combined effect of hydrostatic loading and severe substrate clamping on a thin film. Finally $k'_{\perp}$ in the small slope section decreases as the sample shape changes from bulk (-0.050 $\mu C\,cm^{-2}\,MPa^{-1}$) to thick (-0.025 $\mu C\,cm^{-2}\,MPa^{-1}$) and thin (-0.013 $\mu C\,cm^{-2}\,MPa^{-1}$) films, which may reflect the increase in substrate clamping in general as sample thickness reduces.

We appreciate that with a composition of $Pb(Zr_{0.45}Ti_{0.55})O_3$, our sample is not far from the morphotropic phase boundary on the PZT phase diagram. Experimental results on bulk $Pb(Zr_{1-x}Ti_x)O_3$ samples under hydrostatic pressure show that a phase transition happens for the $x=0.55$ sample when the pressure is in the range of 1.2 GPa.[28] We believe that our sample did not undergo such a phase change in the pressure range (up to 1.5 GPa) that was used for this study, which is consistent with the fact that there was only a single slope for the polarization reduction in pressure.

IV. CONCLUSIONS

We measured the polarization change in a PZT thin film of 130 nm in thickness under hydrostatic pressure. A single linear decrease in the polarization with the increase in applied pressure, similar to the case of in-plane tensile stress, was observed but in a much wider pressure range. By converting both the isotropic loading of hydrostatic pressure and the in-plane stress to equivalent out-of-plane stress, we found that the polarization changes in the cases of in-plane tensile stress and hydrostatic pressure were of the same nature. From the study of the dependence of critical stress on applied maximum switching voltage, we obtained for our sample the material intrinsic critical stress of 1.6 GPa under uniaxial loading and intrinsic coercive voltage of 0.62 V at the stress-free state. Comparison between our results to that of a thicker film and bulk PZT materials was made, showing the decreases of polarization due to ferroelastic switching and material intrinsic lattice distortion and the increase in substrate clamping effect as sample thickness reduces.

ACKNOWLEDGMENTS

This work was partly funded by EPSRC under Grant No. GR/S98412/01.

[1] J. F. Scott and C. Araujo, Science **246**, 1400 (1989).
[2] D. P. Chu, Proceedings of the Third International Conference on Semiconductor Technology, 2004 (unpublished), p. 94.
[3] B. Jaffe, W. R. Cook, Jr., and H. Jaffe, *Piezoelectric Ceramics* (Academic, London, 1971).
[4] G. H. Haertling, J. Am. Ceram. Soc. **82**, 797 (1999).
[5] R. J. Ong, T. A. Berfield, N. R. Sottos, and D. A. Payne, J. Eur. Ceram. Soc. **88**, 2839 (2005).
[6] K. Yao, S. H. Yu, and F. E. H. Tay, Appl. Phys. Lett. **82**, 4540 (2003).
[7] B. J. Koo, Y. J. Song, S. Y. Lee, D. J. Jung, B. H. Kim, and K. Kim, Appl. Phys. Lett. **74**, 2286 (1999).
[8] S. K. Hong, B. Yang, S. H. Oh, Y. M. Kang, and N. S. Kang, J. Appl. Phys. **89**, 8011 (2001).
[9] S. Kobayashi, K. Amanuma, and H. Hada, IEEE Electron Device Lett. **19**, 417 (1998).
[10] W. D. Nix, Metall. Trans. A **20**, 2217 (1989).
[11] R. Yimnirun, Y. Laosiritaworn, and S. Wongsaenmai, J. Phys. D: Appl. Phys. **39**, 759 (2006).
[12] P. M. Chaplya and G. P. Carman, J. Appl. Phys. **90**, 5278 (2001).
[13] C. S. Lynch, Acta Mater. **44**, 4137 (1996).
[14] Q. M. Zhang, J. Zhao, K. Uchino, and J. Zheng, J. Mater. Res. **12**, 226 (1997).
[15] A. Barzegar, D. Damjanovic, N. Ledermann, and P. Muralt, J. Appl. Phys. **93**, 4756 (2003).
[16] G. A. Samara, J. Phys. Chem. Solids **26**, 121 (1965).
[17] G. A. Samara, Ferroelectrics **2**, 277 (1971).
[18] A. M. Grishin, S. I. Khartsev, P. Johnsson, and K. V. Rao, Nanostruct. Mater. **12**, 1141 (1999).
[19] T. Kumazawa, Y. Kumagai, H. Miura, M. Kitano, and K. Kushida, Appl. Phys. Lett. **72**, 608 (1998).
[20] H. D. Kang, W. H. Song, S. H. Sohn, H. J. Jin, S. E. Lee, and Y. K. Chung, Appl. Phys. Lett. **88**, 172905 (2006).
[21] H. Zhu, D. P. Chu, N. A. Fleck, I. Pane, J. E. Huber, and E. Natori, Integr. Ferroelectr. **95**, 117 (2007).
[22] M. B. Kelman, P. C. McIntyre, B. C. Hendrix, S. M. Bilodeau, and J. F. Roeder, J. Appl. Phys. **93**, 9231 (2003).
[23] Q. M. Wang, Y. P. Ding, Q. M. Chen, M. H. Zhao, and J. R. Cheng, Appl. Phys. Lett. **86**, 162903 (2005).
[24] D. R. Franca and A. Blouin, Meas. Sci. Technol. **15**, 859 (2004).
[25] G. A. C. M. Spierings, G. J. M. Dormans, W. G. J. Moors, M. J. E. Ulenaers, and P. K. Larsen, J. Appl. Phys. **78**, 1926 (1995).
[26] W. R. Cook, Jr., D. A. Berlincourt, and F. J. Scholz, J. Appl. Phys. **34**, 1392 (1963).
[27] R. E. Cohen, Nature (London) **358**, 136 (1992).
[28] P. Papet, J. Rouquette, V. Bornand, J. Haines, M. Pintard, and P. Armand, J. Electroceram. **13**, 311 (2004).